JOURNAL OF MATERIALS SCIENCE 27 (1992) 4294–4299

Carbothermal synthesis of titanium nitride

Part II *The reaction sequence*

G. V. WHITE, K. J. D. MACKENZIE, I. W. M. BROWN, M. E. BOWDEN
DSIR Chemistry, Private Bag, Petone, New Zealand
J. H. JOHNSTON
Chemistry Department, Victoria University of Wellington, New Zealand

The conversion of TiO_2 (both anatase and rutile) to TiN by carbothermal reduction in nitrogen was found to proceed by progressive reduction through a homologous series of Magneli phase oxides Ti_nO_{2n-1}, where n has values of 4–10. The next phase to be observed by X-ray diffraction is Ti_3O_5, whose formation from the most stable Magneli phase (Ti_4O_7) is not predicted by the phase diagram, nor by simple thermodynamic calculations. The conversion of triclinic Ti_4O_7 to monoclinic Ti_3O_5 appears to be the slow step in the reaction sequence. Formation of TiN then proceeds directly, apparently without the intervention of Ti_2O_3 or TiO, as usually assumed. A possible cubic oxynitride intermediate was shown by surface analysis to contain no more than 5% oxygen. A small but significant amount of CO is evolved during the formation of Ti_4O_7, with a larger CO evolution occurring during the nitridation of Ti_3O_5. Although no direct mass spectroscopic evidence was found for the formation of C_3O_2, as suggested by previous workers, the present observed weight losses appear to be consistent with this concept. Both the observed reaction sequence and the pattern of CO evolution is consistent with thermodynamic calculations made using a computer program which takes into account the initial nitrogen concentration, and iterates over small temperature intervals.

1. Introduction

In Part I [1] some of the raw material characteristics which influenced the reactivity of titanium oxides and carbon in the formation of titanium nitride were identified in a broad survey of a number of titanias and carbons. To quantify the reactivity, a novel X-ray analytical method was developed, in which the internal standard (Al_2O_3) was added prior to heating the reactant mixture. On the basis of these results, two rutiles and four anatases were selected for more detailed studies of the reaction sequence.

The overall reaction equation for carbothermal reduction and nitridation of TiO_2 can be written [2]

$$TiO_2 + 2C + \tfrac{1}{2}N_2 \rightarrow TiN + 2CO \qquad (1)$$

However, it has long been clear that the reaction involves a number of steps, some of which overlap. Ličko *et al.* [3] summarized these as

(a) initial reduction of TiO_2 to the lower oxides Ti_3O_5, Ti_2O_3 and finally TiO. The nitrogen atmosphere takes no part in these initial reactions;

(b) substitution of oxygen by nitrogen in the cubic TiO. In concluding that TiO is the immediate precursor for TiN, Ličko *et al.* [3] quote work published 60 years ago by Umezu [4].

Although Equation 1 suggests CO to be the only gaseous reaction product, some workers have also detected smaller amounts of CO_2 in the effluent gas stream [5]. Furthermore, when the evolved gas is rapidly removed by reduced pressure [5], or by increasing the nitrogen flow [6], the reaction rate is decreased, suggesting that the CO and CO_2 are actively participating in the reaction rather than occurring simply as by-products. It is suggested [6] that CO formed by initial reduction of TiO_2 also acts as a reducing agent

$$CO + 3TiO_2 \rightarrow Ti_3O_5 + CO_2 \qquad (2)$$

The CO_2 is then reduced

$$CO_2 + C \rightarrow 2CO \qquad (3)$$

Although Lyubimov *et al.* [6] support the concept of progressive reduction to lower oxides, they failed to observe Ti_2O_3 and TiO as intermediates in their experiments, explaining this in terms of crystallographic factors which favoured the direct conversion of Ti_3O_5 to a cubic oxycarbonitride.

The failure by many workers to detect significant amounts of CO_2 in the effluent gases has led to a study using accurate analysis and weight measurement [7]. The results have been interpreted in terms of the initial formation of C_3O_2 which then acts as a reducing agent by supplying further accessible carbon

$$6TiO_2 + 3C \rightarrow 2Ti_3O_5 + C_3O_2 \qquad (4)$$

$$C_3O_2 \rightarrow 2CO + C \qquad (5)$$

Although mass spectrometric evidence for gaseous C_3O_2 was not found, carbon condensed on the cooler parts of the furnace tube [7]. A thermodynamic analysis also predicted the formation of small amounts of C_3O_2 [8].

The aim of this work was to investigate the carbothermal reaction sequence in both rutile and anatase, with particular attention to the points on which the previous literature disagrees, namely

(i) the formation sequence of the lower oxides and the identity of the TiN precursor; and

(ii) the nature and role of the gaseous species involved.

X-ray powder diffraction was used to identify the crystalline phases present at the various stages of the reaction, and the corresponding gas atmosphere was continuously monitored. The experimental results were compared with predictions arising from thermodynamic calculations.

2. Experimental procedure

The two rutiles and four anatases used in this and the subsequent kinetic studies (Part III [9]) are described in Part I [1] in Table I. The carbon used in all these experiments is designated C8 in that Table. Mixtures of TiO_2 and powdered carbon (molar ratio 1 : 4) were heated in flowing oxygen-free nitrogen ($0.1\ l\,min^{-1}$) at a linear heating rate of $5\,°C\,min^{-1}$ in an electric tube furnace. At various temperatures the samples were quenched under nitrogen and examined by X-ray powder diffraction (XRD) as previously described [1].

Analysis of the effluent gas stream was by infrared spectroscopy, using a gas cell in a Perkin–Elmer 337 spectrophotometer set at the appropriate wavelength for CO. Although CO_2 was sought by this technique, it was of variable concentration, and generally not above the background level. Some heatings were made using a quadrupole mass spectrometer (Extranuclear Inc.) to monitor the composition of the effluent gas.

Thermogravimetric analysis (TG) and differential thermal analysis (DTA) was carried out under a dynamic nitrogen atmosphere ($60\ ml\,min^{-1}$) at a heating rate of $10\,°C\,min^{-1}$, using a Stanton Redcroft TG770 thermobalance and a Stone Model 202 differential thermal analyser.

Thermodynamic modelling was carried out using the computer program SOLGASMIX [10]. The program calculates the equilibrium amounts of all the condensed species, the partial pressures of the gas species, the mole fractions of all species in the condensed phase and the activities of the species in all mixtures by an iterative free-energy minimization method [10]. The thermodynamic data were from Chase [11] and Barin *et al.* [12, 13].

3. Results and discussion

3.1. Phases formed during the reaction sequence

Fig. 1 shows semischematically the relative amounts of the various phases formed from anatase and carbon heated at 800–1300 °C in a dynamic nitrogen atmosphere. In this diagram, the intensities of major XRD peaks are used as a measure of the relative amounts present. In the initial stage of the reaction sequence, conversion to rutile begins at the usual temperature (about 950 °C). As the temperature is increased, the rutile becomes progressively oxygen deficient, as evidenced by a darkening of its colour, but retains the rutile XRD pattern. According to the titanium oxide phase diagram [14], further loss of oxygen should result in the formation of a homologous series of lower oxides called Magneli phases. These have the general formula Ti_nO_{2n-1}, with n having values of 4–10, although phases with n up to 38 have been reported [15]. The Magneli phases are triclinic, with structures consisting of slabs of a rutile-like structure n octahedra thick, separated by a boundary region where octahedra from adjacent slabs share edges, corners and faces in a corundum-like structure [16]. The reduction of one oxide in the series to the next involves the loss of one TiO_6 octahedral layer from each rutile-like slab. Fig. 1 shows that the only Magneli phase observed in the present quenched samples was the most highly reduced member, Ti_4O_7. Because the stability of the Magneli phases increases with decreasing n [17], only the most stable of these phases was observed here, appearing at the expense of rutile at about 1000 °C and disappearing by 1100 °C (Fig. 1). The JCPDS reference patterns for Ti_4O_7 and the other Magneli phases are generally quite poor, extending over a limited range of lattice spacings, and with visually estimated intensities, which, although in limited agreement with the present experimental powder patterns, are insufficiently good to engender confidence in the identification of Ti_4O_7 in these samples (Fig. 2). For this reason, the powder pattern for Ti_4O_7 was calculated from the crystal structure of Marezio and Dernier [18] using the computer program DISPOW [19]. The agreement between the calculated and the observed patterns of Ti_4O_7 represents a considerable improvement over the JCPDS pattern and confirms the presence of Ti_4O_7 in the fired samples.

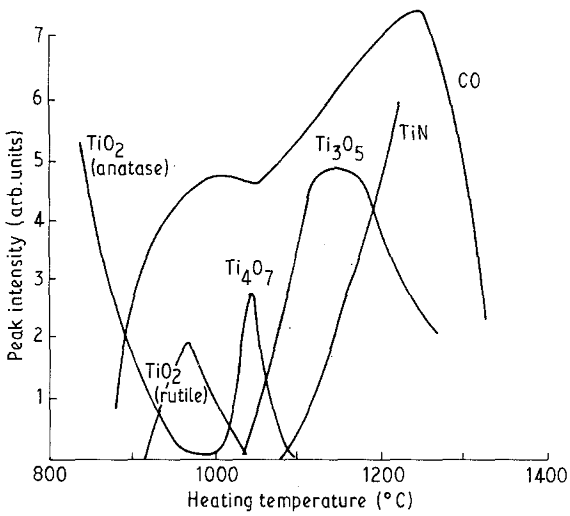

Figure 1 Semischematic representation of the phases formed during heating in nitrogen ($0.1\ l\,min^{-1}$) of a typical anatase–carbon mixture (molar ratio 1 : 4) and the evolution curve for CO, monitored by infrared spectroscopy. Heating rate $5\,°C\,min^{-1}$.

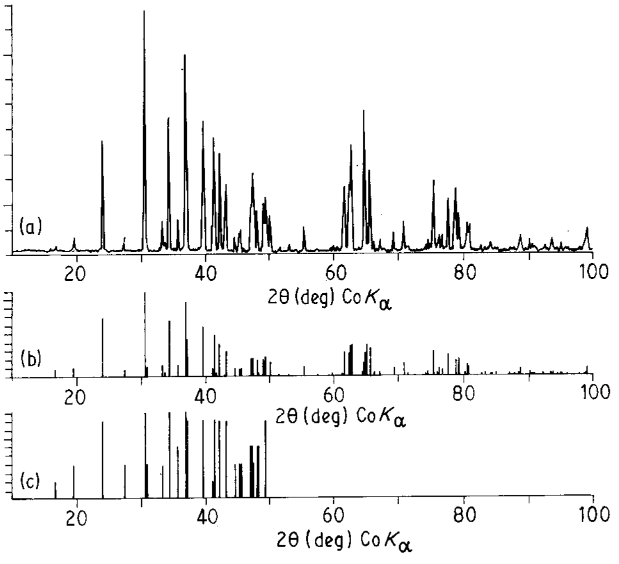

Figure 2 (a) Observed X-ray powder pattern of Ti_4O_7, compared with (b) powder pattern calculated from the crystal structure [18] (present work), and (c) the JCPDS reference pattern (card no. 18-1402).

According to the phase diagram [14], further loss of oxygen should result in the formation of Ti_2O_3 and cubic TiO. In the presence of nitrogen, the latter should form cubic TiN either by direct substitution of nitrogen for oxygen or via an intermediate oxynitride. In fact, no evidence was found of either Ti_2O_3 or TiO in numerous experiments; the phase which preceded the appearance of TiN, and frequently occurred together with it, had an X-ray pattern corresponding most closely to monoclinic Ti_3O_5 (JCPDS card 23-606). The formation of Ti_3O_5 is consistent with results reported by Lyubimov *et al.* [20], who identified two Ti_3O_5-like phases found in the products of carbothermal reduction of Ti_2O_3 and TiO as titanium oxynitrides. Discrepancies between the intensity ratios of the present patterns and the JCPDS card, are significant, especially in the low-angle peak at $d = 0.49$ nm. This could indicate a degree of substitution of oxygen by nitrogen as suggested by Ličko *et al.* [3], although a new calculated powder pattern for Ti_3O_5 [21] resembles the present patterns more closely than JCPDS 23-606. Thus, the present patterns do not necessarily imply the presence of nitrogen. The Ti_3O_5 phase first appears above 1050 °C and decreases in intensity with the growth of TiN above 1100 °C (Fig. 1).

The cubic lattice parameter of the TiN formed at 1090–1250 °C is 0.424 nm, in reasonable agreement with tabulated values for TiN (0.4213–0.4235 nm), but this does not, however, exclude the possibility of a significant oxygen content in this phase, because TiO has almost the same lattice parameter (0.4168–0.4201 nm); up to 40% substitution of nitrogen in TiN by oxygen can occur without change in the TiN lattice parameter [22]. Because the lattice parameter measurements are not a sensitive indicator of oxygen impurities in TiN, the sample fired at 1250 °C was subjected to oxygen analysis by particle-induced gamma-ray emission (PIGME). The resulting oxygen content was only about 5%, and may have been influenced by oxygen adsorbed on the surface of the particles, because PIGME is a surface analysis technique.

On firing the TiN product to considerably higher temperatures (1500 °C for 4 h), the lattice parameter is increased to 0.428 nm, due to incorporation of carbon in the lattice. According to the relationship between lattice parameter and carbon content reported by Shimada *et al.* [23], this corresponds to a composition of $TiC_{0.5}N_{0.5}$.

3.2. Thermal analysis of TiO_2–carbon mixtures in nitrogen

A typical set of thermal analysis curves for a TiO_2–carbon mixture in nitrogen is shown in Fig. 3. The TG curve (Fig. 3a) suggests that the weight loss during the reaction occurs in several stages, which are more apparent from the DTG curve (Fig. 3b). The small weight loss at 100 °C is associated with the endothermic loss of adsorbed water, as also shown by the DTA trace (Fig. 3c). The small weight loss at about 730 °C which is also seen as an endotherm in the DTA

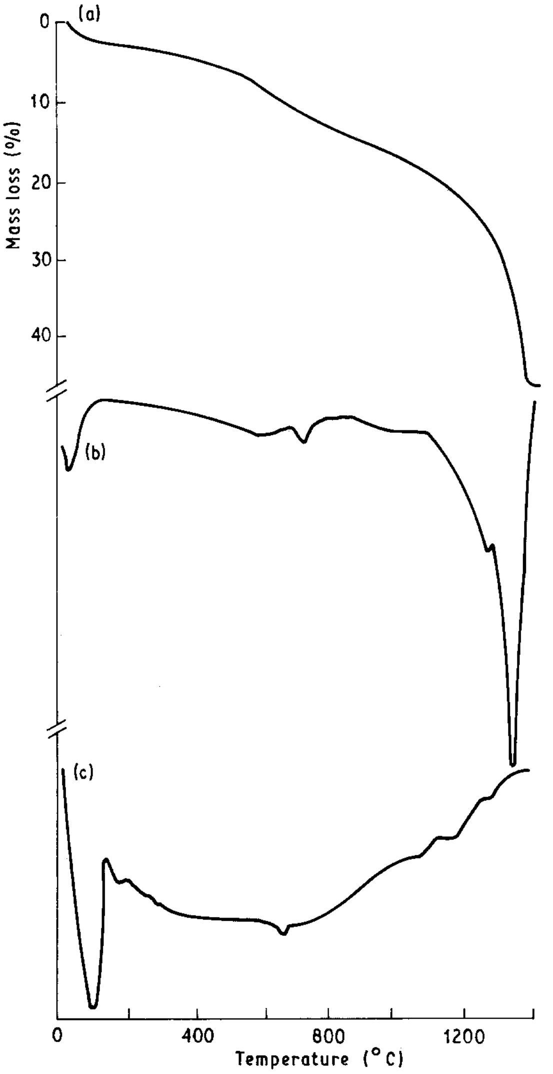

Figure 3 Typical thermal analysis curves for an anatase A1–carbon C1 mixture (molar ratio 1:4) in nitrogen (60 ml min^{-1}), heating rate 10 °C min^{-1}. (a) TG curve, (b) DTG curve, (c) DTA curve.

trace, results from the decomposition of $CaCO_3$ impurity in the carbon. The two higher temperature weight loss stages appear to be related to the formation of Ti_3O_5 from Ti_4O_7 and of TiN from Ti_3O_5, respectively; at a slower heating rate, these DTG peaks occur at 1190 and 1240 °C, approximately the temperatures when these phases were first observed by XRD in quenched samples. The DTA counterpart of the large high-temperature weight loss is the three very small DTA endotherms, at 1080, 1170 and 1280 °C which are probably associated with these reactions. The formation of Ti_3O_5 from Ti_4O_7 and of TiN from Ti_3O_5 is endothermic (76 and 281 $kJ\,mol^{-1}$, respectively [24, 25], but the formation of TiO is strongly exothermic, further ruling out this species as an intermediate in the reaction.

3.3. Comparison of the reaction sequence with thermodynamic predictions

The thermodynamic feasibility of the various possible reactions occurring during carbothermal reduction of TiO_2 in nitrogen over the temperature range of present experiments was calculated using the thermodynamic data of Weeks and Block [24] and Robie *et al.* [25]. Although the comparison of thermodynamic data with the present experimental results is not strictly valid because the former relate to equilibrium conditions which do not necessarily exist in these experiments, some interesting points emerge.

Of all the possible phases which could form from TiO_2 below 1150 °C with the evolution of CO, Ti_4O_7 has the most negative free energy of reaction, followed by Ti_3O_5, Ti_2O_3, TiO and TiC (Fig. 4). Thus, below 1150 °C, the formation of Ti_4C_7 is the thermodynamically favoured reaction (although the data for the higher Magneli phases are not available). Above ~ 1150 °C, TiN is the thermodynamically favoured phase (Fig. 4).

Similar calculations for the further reactions of Ti_4O_7 predict that it should form TiN directly at temperatures above 1080 °C; the free energy of formation of Ti_3O_5, Ti_2O_3, or TiO from Ti_4O_7 is positive over this entire temperature range. This prediction is at variance with the experimental results, possibly due to the greater reactivity of the carbon used in this work, by comparison with the graphite used as the thermodynamic reference phase. Furthermore, the thermodynamic calculations indicate that if Ti_3O_5 or Ti_2O_3 were to form they would be unstable with respect to the formation of TiN. Thus, although these calculations correctly predict the stability of Ti_4O_7 below 1150 °C, they do not suggest the formation of Ti_3O_5 as an intermediate in the formation of TiN, as observed in these experiments.

The SOLGASMIX computer program provides a more sophisticated thermodynamic model of the system, simultaneously taking into account the effect of the entire assemblage of gaseous species as well as the condensed phases. In these calculations, the initial composition was set at 2 mol TiO_2, 5 mol C, and 1,3 and 5 mol N_2, with temperature intervals as small as 5 K. The sequence of condensed phases thus calculated for 3 mol N_2 is shown in Fig. 5. The phase sequence of Fig. 5 is strikingly similar to the experimental results (Fig. 1), predicting the formation of Ti_4O_7 and Ti_3O_5 as intermediates in the formation of TiN from TiO_2. A similar result is found for 1 and 5 mol N_2, but at the lower nitrogen content, the formation of some TiC at the expense of TiN is predicted above 1060 °C, due to the presence of the excess carbon assumed in the calculations. The transitory

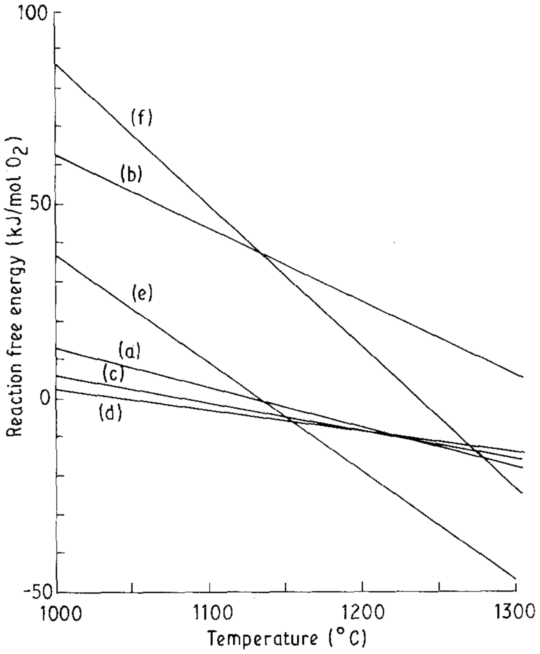

Figure 4 Temperature dependence of the free energies of the possible carbothermal reduction and nitridation reactions of TiO_2

(a) $TiO_2 + \frac{1}{2}C \rightarrow \frac{1}{2}Ti_2O_3 + \frac{1}{2}CO$

(b) $TiO_2 + C \rightarrow TiO + CO$

(c) $TiO_2 + \frac{1}{3}C \rightarrow \frac{1}{3}Ti_3O_5 + \frac{1}{3}CO$

(d) $TiO_2 + \frac{1}{4}C \rightarrow \frac{1}{4}Ti_4O_7 + \frac{1}{4}CO$

(e) $TiO_2 + 2C + \frac{1}{2}N_2 \rightarrow TiN + 2\,CO$

(f) $TiO_2 + 3C \rightarrow TiC + 2\,CO$

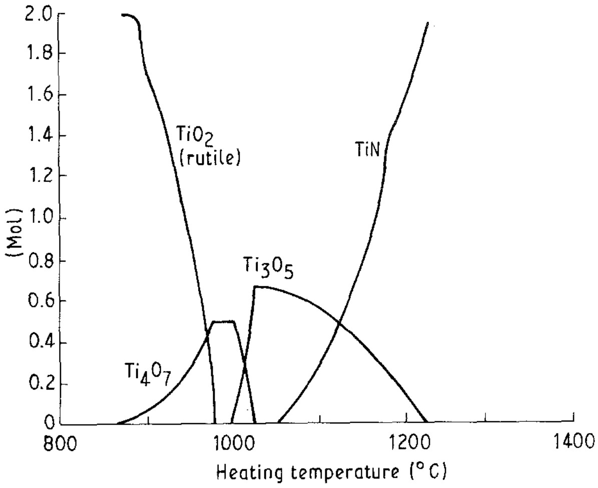

Figure 5 Equilibrium phases formed from TiO_2–C mixtures (molar ratio 2:5) in 3 mol N_2, as a function of temperature, calculated by the SOLGASMIX program.

appearance of a small amount of Ti_2O_3 is also predicted at about 1015 °C. At the lowest nitrogen level, a final equilibrium between TiC and TiN is reached at 1130 °C, corresponding to a carbonitride composition of $TiC_{0.5}N_{0.5}$. No TiO was predicted at the nitrogen contents assumed in these calculations.

3.4. The nature of the gaseous species in the reaction

Changes in the CO level during the reaction sequence are plotted in Fig. 1. This indicates that CO evolution occurs during the initial reduction of the Magneli phases, and again during the later stages of the reaction. A minimum in the CO evolution coincides with the conversion of Ti_4O_7, the most stable of the Magneli phases, to Ti_3O_5. The two stages of CO evolution may be written

$$4TiO_2 + C \rightarrow Ti_4O_7 + CO \qquad (6)$$

The Ti_4O_7 converts to Ti_3O_5, which then nitrides

$$Ti_3O_5 + 5C \xrightarrow{N_2} 3TiN + 5CO \qquad (7)$$

These equations are consistent with the relatively larger CO evolution associated with the latter stage. The pause in the reaction indicated by the minimum in CO evolution suggests that the transformation from Ti_4O_7, the lowest member of the Magneli series, to Ti_3O_5 (a different structure) may be the slow step in the sequence.

Mass-spectrometric examination of the evolved gases was hampered by continual blockages of the bleed valve, possibly due to deposited carbon such as found by Lyubimov *et al.* [7] and ascribed to the disproportionation of C_3O_2. Apart from CO and nitrogen (mass 28), the only other gas species of interest was CO_2, which was detected in small but variable amounts. Further information on the possible formation of C_3O_2 may be derived from the weight losses recorded during the reaction. If, as suggested [7], C_3O_2 is generated during the reaction and evolved into the gas stream, it will be lost from the sample, which will therefore show a different weight loss. The two possibilities may be written

$$TiO_2 + 4C + 1/2N_2 \rightarrow TiN + 2CO\uparrow + 2C \quad (8)$$

(theoretical weight loss = 33%)

$$TiO_2 + 4C + 1/2N_2 \rightarrow TiN + C_3O_2\uparrow + C \quad (9)$$

(theoretical weight loss = 42%)

Although the present weight losses measured for a number of samples were variable, they were all greater than 33%, and much nearer 42%, the maximum value which was recorded for one of the rutiles reacted for 1 h at 1500 °C. Although these results appear to be more consistent with Equation 9, they should be viewed with some caution, because the presence of air trapped in the powder samples and the formation of a small amount of oxide on the surface on the powdered bed by the action of oxygen contaminants will influence the weight losses.

The SOLGASMIX program can be used to predict the equilibrium CO contents at various temperatures throughout the range. Because these equilibrium results cannot be compared directly with the dynamic results obtained by EGA (Fig. 1), an attempt was made to synthesize an evolved CO curve from the equilibrium CO data. The procedure involves subtracting the equilibrium CO concentrations at adjacent temperatures, dividing by the temperature interval and assigning the result to the higher temperature. These data were then smoothed, fitted to a curve by a tension spline program and differentiated to give a graph of rate of change of CO equilibrium with temperature. Fig. 6 shows the resulting calculated curve for an initial nitrogen concentration of 3 mol, together with the experimental curve for comparison. The agreement between the two curves is surprisingly good; both show a small CO peak associated with reduction to Ti_4O_7 followed by a larger CO evolution resulting from nitride formation (Fig. 6).

4. Conclusions

The initial stages of carbothermal reduction of anatase and rutile in a nitrogen atmosphere involve the progressive reduction of the TiO_2 through a homologous series of Magneli phase oxides of general formula Ti_nO_{2n-1} where n has values 4–10. Only the most stable of these oxides, Ti_4O_7 was observed by XRD. The formation of the next phase to be observed, Ti_3O_5, involves a change of structure from that of the Magneli series, and its appearance is not predicted by the phase diagram nor by simple thermodynamic considerations. The appearance of Ti_3O_5 but not Ti_2O_3 and TiO as intermediates of finite lifetime in the formation of TiN is at variance with Ličko *et al.* [3] but confirms findings of Lyubimov *et al.* [6], whose suggestion that this phase may also contain some nitrogen substitution cannot be excluded by the present results. TiN forms directly from Ti_3O_5 possibly via a cubic oxynitride which, however, was found by a surface analysis method to contain no more than 5%

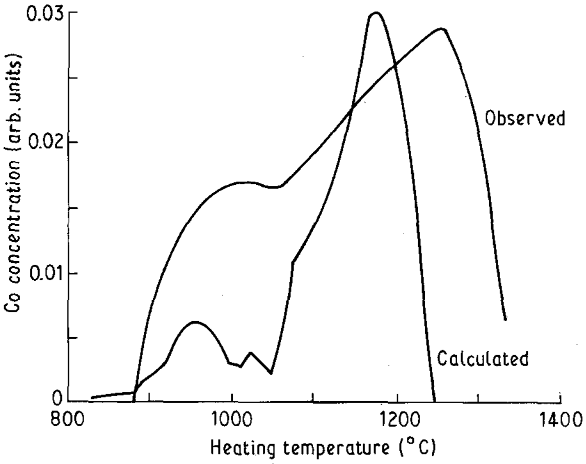

Figure 6 Observed CO evolution from TiO_2–C mixture as a function of heating temperature, compared with the curve derived from thermodynamic calculations by the SOLGASMIX program for a system containing 3 mol N_2.

oxygen. At much higher temperatures (1500 °C), carbon is incorporated in the nitride lattice, replacing up to 50% of the nitrogen content.

The major gaseous species observed in the reaction atmosphere is CO, which is evolved during the progressive reduction of the Magneli phases, and again in greater concentration during the nitridation of Ti_3O_5. A pause in the CO evolution suggests that the formation of Ti_3O_5 from Ti_4O_7 may be the slow step in the reaction. Direct evidence for the formation of C_3O_2 as postulated by Lyubimov *et al.* [7] was not found, although observed weight losses during the reaction appear to be consistent with such a mechanism. No evidence was found for significant participation of CO_2 in the reaction sequence.

Acknowledgements

We are indebted to Dr L. Parker, Dr D. Rodgers and Dr N. Tapp for assistance with the thermal analysis, to Dr G. Coote, for the PIGME analyses, and to Mr J. Sjöberg, Chalmers Technical University, Sweden, for assistance with the SOLGASMIX calculations.

References

1. G. V. WHITE, K. J. D. MACKENZIE and J. H. JOHNSTON, *J. Mater. Sci.* **27** (1992) 4287.
2. E. K. KLEEPSIES and T. A. HENDRIE, US Bur. Mines Report 6447 (1964).
3. T. LIČKO, V. FIGUS and J. PÚCHYOVÁ, *J. Eur. Ceram. Soc.* **5** (1989) 257.
4. S. UMEZU, *Proc. Imp. Acad.* (*Tokyo*) **7** (1931) 353.
5. G. D. BOGMOLOV, V. D. LYUBIMOV and G. P. SHVERKIN, *J. Appl. Chem. USSR* **44** (1971) 1227.
6. V. D. LYUBIMOV, T. V. SHESTAKOVA, G. P. SHVERKIN, S. I. ALYAMOVSKII and YU. G. ZAINULIN, *Inorg. Mater.* **13** (1977), 46.
7. V. D. LYUBIMOV, G. P. SHVERKIN, YU. D. ALFONIN, T. A. TIMOSCHUK, V. N. SHALAGINOV, M. V. KALACHEVA and S. I. ALYAMOVSKII, *ibid.* **49** (1984) 49.
8. V. D. LYUBIMOV, G. K. KOISEEV and T. A. TIMOCHUK, *ibid.* **21** (1985) 1158.
9. G. V. WHITE, K. J. D. MACKENZIE, I. W. M. BROWN and J. H. JOHNSTON, *J. Mater. Sci.* **27** (1992) 4300.
10. G. ERIKSSON, *Chem. Scripta* **8** (1975) 100.
11. M. W. CHASE (ed.), "JANAF Thermochemical Tables", 3rd Edn (American Chemical Society, American Institute for Physics, and National Bureau of Standards, 1986).
12. I. BARIN and O. KNACKE, "Thermochemical Properties of Inorganic Substances" (Springer-Verlag, Berlin, 1973).
13. I. BARIN, O. KNACKE and O. KUBASCHEWSKI, "Supplement to Thermochemical Properties of Inorganic Substances" (Springer-Verlag, Berlin, 1977).
14. P. G. WAHLBECK and P. W. GILLES, *J. Amer. Ceram. Soc.* **49** (1966) 180.
15. L. A. BURSILL, B. G. HYDE, O. TERASAKI and D. WATANABE, *Phil. Mag.* **20** (1969) 347.
16. S. ANDERSSON and L. JAHNBERG, *Arkiv. Kemi* **21** (1964) 413.
17. R. R. MERRITT, B. G. HYDE, L. A. BURSILL and D. K. PHILP, *Phil. Trans. R. Soc. Lond. Ser. A* **274** (1973) 627.
18. M. MAREZIO and P. D. DERNIER, *J. Solid State Chem.* **3** (1971) 340.
19. "DISPOW", written by A. C. Larson, F. L. Lee, Y. Le-Page and E. J. Gabe, Chemistry Division, Ottawa, Canada (1983).
20. V. D. LYUBIMOV, T. V. SHESTAKOVA, G. P. SHVERKIN and S. I. ALYAMOVSKII, *Russ. J. Inorg. Chem.* **22** (1977) 1620.
21. M. E. BOWDEN, personal communication (1989).
22. L. E. TOTH, "Transition Metal Carbides and Nitrides" (Academic Press, New York, 1971).
23. M. SHIMADA, T. SUZUKU and M. KOIZUMI, *Mater. Lett.* **1** (1983) 175.
24. C. E. WEEKS and F. E. BLOCK, *US Bur. Mines Bull.* **605** (1963).
25. R. A. ROBIE, B. S. HEMINGWAY and J. R. FISHER, *US Geol. Surv. Bull.* **1452** (1978).

Received 23 April
and accepted 5 August 1991